

## Single-Event Hanbury-Brown-Twiss Interferometry

CHEUK-YIN WONG

*Physics Division, Oak Ridge National Laboratory, Oak Ridge, TN 37830, U.S.A.  
Department of Physics, University of Tennessee, Knoxville, TN 37996, U.S.A.  
wongc@ornl.gov*

WEI-NING ZHANG

*Department of Physics, Dalian University of Technology, Dalian, Liaoning 116024, China  
Department of Physics, Harbin Institute of Technology, Harbin, Heilongjiang 150006, China  
weiningzh@hotmail.com*

Received (received date)

Revised (revised date)

Large spatial density fluctuations in high-energy heavy-ion collisions can come from many sources: initial transverse density fluctuations, non-central collisions, phase transitions, surface tension, and fragmentations. The common presence of some of these sources in high-energy heavy-ion collisions suggests that large scale density fluctuations may often occur. The detection of large density fluctuations by single-event Hanbury-Brown-Twiss interferometry in heavy-ion collisions will provide useful information on density fluctuations and the dynamics of heavy-ion collisions.

### 1. Introduction

Large spatial density fluctuations in high-energy heavy-ion collisions can come from many sources. Some of these sources are expected to be quite common in high-energy heavy-ion collisions and consequently large scale density fluctuations may often occur. It is of great interest to examine the sources of large density fluctuations and to find ways for their detection so as to obtain useful information on the collision dynamics<sup>1,2,3,4,5,6</sup>.

Among the many different ways to study a quark-gluon plasma, intensity interferometry (HBT interferometry) is one of the experimental tools to examine the space-time density distribution of the produced matter<sup>7</sup>. The usual application of the HBT interferometry uses pairs of identical particles from many events (multi-event analysis) of similar general characteristics to study the (averaged) space-time configuration. Because of the difference in initial conditions in different collision events, different collisions will lead to different density fluctuations for some degrees of freedom while retaining similar fluctuations for some other degrees of freedom. An average over many events in a standard HBT analysis will lead to a distribution with suppressed fluctuations in event-dependent degrees of freedom but will retain those fluctuations in event-independent degrees of freedom. The proposed single-

event HBT analysis, if it can be carried out with sufficient accuracy, allows the examination of the full characteristics of large scale density fluctuations without suppression. The observation of HBT interferometry in atomic systems also make it interesting to examine the interference pattern in systems with large macroscopic density fluctuations<sup>8,9</sup>.

If the statistics of identical bosons turns out to be insufficient for single-event HBT analyses using presently available detectors, it will be of interest to carry out few-event HBT analyses to examine event-independent density fluctuations. The few-event analysis will however require a good theoretical understanding of the single-event HBT interferometry.

With the example of a granular density distribution to indicate the type of correlations one can get in a large scale density fluctuation, we shall show that the correlation function of a highly fluctuating density distribution is likewise highly fluctuating, with maxima and minima at locations which depend on the relative coordinates of the density centers. These local maxima and minima arise from the constructive and destructive interferences of identical bosons originating from two different centers. Their interference patterns therefore provide useful information on highly fluctuation density distributions in high-energy heavy-ion collisions.

## 2. Sources of Large Density Fluctuations

In many simulations of the heavy-ion collisions on an event-by-event basis, the initial transverse energy density is far from being uniform. It exhibits large transverse density fluctuations with a large peak-to-valley ratio<sup>10,11,12</sup>. A number of transverse density ‘lumps’ are clearly visible in the initial transverse density distribution of the produced matter in Fig. 21 of Ref. [10] or Fig. 4 of Ref. [11] shown in Fig. 1(a).

Because of Lorentz contraction, the longitudinal length of the produced matter is much smaller than the transverse length. Initially as depicted in Fig. 1(a), density fluctuations in the transverse plane manifest as a number of transverse lumps<sup>10,11</sup>. The subsequent longitudinal expansion proceeds much faster than the transverse expansion, as pointed out by Landau and Belenkii<sup>13</sup>. The expanding matter develops into tubes [Fig. 1(b)] and the density of matter in the tube decreases as a function of the proper time. The sausage instability leads to the break-up of the tube of matter into many approximately equal spherical droplets<sup>5</sup> depicted in Fig. 1(c), as in the break-up of toroidal liquid drops<sup>14</sup>.

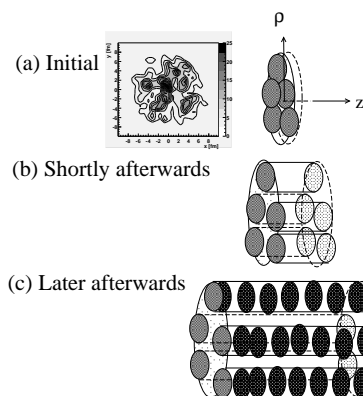


Fig. 1. The scenario in a central high-energy heavy-ion collision.

Another initial transverse density distribution occurs in non-central collisions of two approximately equal size nuclei. In these collisions, while the spectator matter proceeds forward, the participants collide and interact. The pion-emitting source produced by the participants may retain part of the initial momenta in different spatial regions. If the produced matter constituents retain a large fraction of the initial momenta, they can be approximately idealized as two pion emitting clusters as shown in Fig. 2a. On the other hand, if a significant fraction of the participant matter in the overlapping region is stopped while the more peripheral constituents moves in their original directions, the pion emitting source can be approximated as consisting of three clusters as in Fig. 2b. Interference of identical pions emitted from either two or three clusters will exhibit features associated with these spatial configurations.

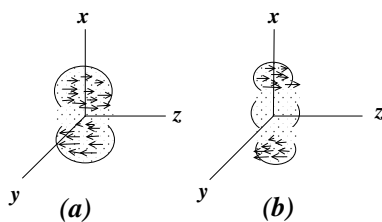


Fig. 2. Possible configurations of the pion-emitting source after a non-central collision.

Another source of density fluctuation arises from the occurrence of first-order phase transition, as was first pointed out by Witten<sup>15</sup> and examined by many workers<sup>1,2,3,4,5,16</sup>. According to such a description, incipient bubbles of low-density matter (hadrons) are formed in some local regions in a nearly static quark-gluon plasma, as the local temperature decreases below the phase transition temperature. The coalescence of these bubbles leads to bubbles of larger radii. As the system cools further, the fraction of matter in the low-density bubbles will become greater than the fraction of high-density matter (QGP), and the high-density matter will turn into lumps in the low-density matter background. The density of such a configuration is highly fluctuating.

Still another source of density fluctuation arises from the effects of surface tension during the evolution of the strongly-interacting matter. Because the QGP and the hadron matter are strongly interacting dense media, a surface tension arises at a boundary due to the presence of a strong interaction in the dense phase on one side of the boundary and the absence (or weakening) of the strong interaction with no density (or diminishing density) on the other side. This imbalance of the forces acting on different parts at the boundary leads to the surface tension, and the detail profile of the boundary may depend on the nature and the order of phase transition. Due to the presence of this surface tension, there may be the instability against surface shape changes that favors the formation of surfaces of smallest areas in different local regions. Such a tendency lead to large spatial density fluctuations. The end product may be the multi-fragmentation of the strongly-interacting matter. Multi-fragmentation has been observed in intermediate energy heavy-ion collisions<sup>17</sup>.

### 3. Detection of Large Density Fluctuations by Single-Event HBT Interferometry

In order to understand how the features of the correlation function may be affected by the presence of large density fluctuations, it is worth studying the correlation function of identical particles of momentum  $k_1$  and  $k_2$  with  $q = k_1 - k_2$  and  $P = (k_1 + k_2)/2$  for an idealized chaotic droplet sources<sup>3</sup>. There is a relation between the two-boson correlation function and the Fourier transform of the source density  $\rho(x; k_1, k_2)$ , which we assume to be independent of  $q$ ,

$$C(q, P) = 1 + \left| \int dx e^{iq \cdot x} \rho(x, P) \right|^2. \quad (1)$$

For brevity of notation, we shall leave the label  $P$  implicit and understood.

We consider a density distribution of  $N$  droplets of the type

$$\rho(x) = A \sum_{j=1}^N \rho_j(x), \quad (2)$$

where  $\rho_j$  is the density distribution of the  $j$ -th droplet, and  $A$  is a normalization constant such that the total density  $\rho(x)$  is normalized to unity as  $\int dx \rho(x) = 1$ . We can consider the  $j$ -th droplet to have particle emission time centering at  $T_j$ , to be localized initially at  $\mathbf{R}_j$  with standard deviations  $\sigma_j$  and  $\tau_j$ , and to move with a velocity  $\mathbf{v}_j$ ,

$$\rho_j(t, \mathbf{r}) = \frac{e^{-(\mathbf{r}-\mathbf{R}_j-\mathbf{v}_j t)^2/2\sigma_j^2} e^{-(t-T_j)^2/2\tau_j^2}}{(\sqrt{2\pi}\sigma_j)^3 \sqrt{2\pi}\tau_j}. \quad (3)$$

The correlation function is then

$$C(q) = 1 + \left| A \sum_{j=1}^N \exp \left\{ i\mathbf{q} \cdot \mathbf{R}_j - i(q_0 - \mathbf{q} \cdot \mathbf{v}_j)T_j - \frac{\sigma_j^2 \mathbf{q}^2}{2} - \frac{\tau_j^2 (q_0 - \mathbf{q} \cdot \mathbf{v}_j)^2}{2} \right\} \right|^2 \quad (4)$$

In order to get a clear insight into the most important features of the correlation function, we consider the simple case where the density distributions of all droplets are the same so that  $\sigma_j = \sigma$  and  $\tau_j = \tau$  for all  $j$ . In this simple case,  $A = 1/N$  and the correlation function can be easily evaluated to give

$$C(q) = 1 + \frac{e^{-\sigma^2 \mathbf{q}^2}}{N^2} \left[ \sum_{j=1}^N e^{-\tau^2 (q_0 - \mathbf{q} \cdot \mathbf{v}_j)^2} + 2 \sum_{\substack{j,k=1 \\ j>k}}^N e^{-\frac{\tau^2}{2} [(q_0 - \mathbf{q} \cdot \mathbf{v}_j)^2 + (q_0 - \mathbf{q} \cdot \mathbf{v}_k)^2]} \cos \Delta_{jk} \right] \quad (5)$$

$$\Delta_{jk} = -q \cdot (X_j - X_k) - \mathbf{q} \cdot (\mathbf{v}_j T_j - \mathbf{v}_k T_k), \quad X_j = (T_j, \mathbf{R}_j). \quad (6)$$

Thus, the correlation function  $C(q)$  has maxima at  $\Delta_{jk} \sim 2n\pi$ , and minima at  $\Delta_{jk} \sim (2n-1)\pi$ , with  $n = 1, 2, 3, \dots$ . Numerical examples with  $N = 4$  and  $N = 8$  static droplets are shown in Figs. 1 and 2 of Ref. [3]. The number of correlation function maxima for 8 droplets is greater than the number of maxima for 4 droplets.

The smaller the number of droplets, the greater will be the magnitude of fluctuations, as can be easily deduced from Eq. (5). Previously, we examine the two-pion interferometry for a granular source of quark-gluon plasma droplets and found that the granular model of the emitting source may provide an explanation to the RHIC HBT  $R_{\text{out}}/R_{\text{side}}$  puzzle<sup>2,5</sup>. We also investigate two-pion Bose-Einstein correlations of many droplets in single-event measurements. We find that the distribution of the fluctuation between correlation functions of the single- and mixed-events provide useful signals to detect the granular structure of the source<sup>4</sup>.

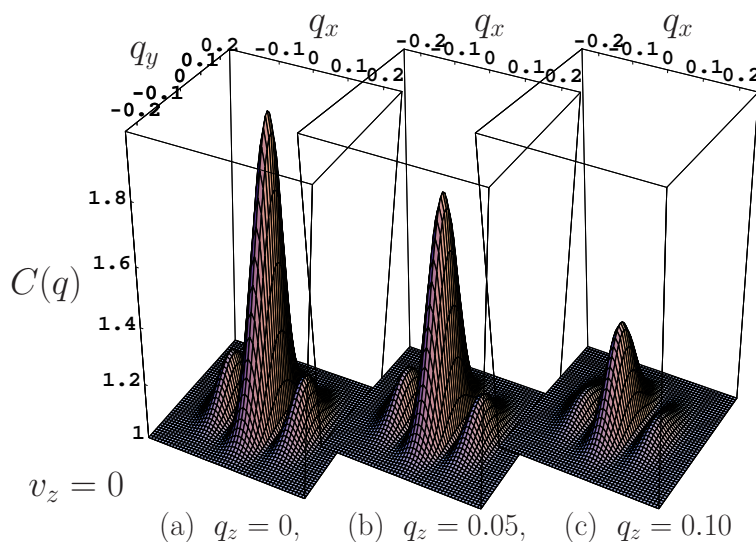


Fig. 3. The correlation function for a two static droplet source.

The case of  $N = 2$  presents an interesting example of the fluctuation of the HBT correlation functions. For the case of two static droplets of  $\sigma = 2$  fm at an approximately touching configuration with a separation of  $2\sqrt{5}\sigma = 8.84$  fm in the  $x$  direction, Figs. (3a) give the correlation functions  $C(\mathbf{q})$  at  $q_0 = 0$  as a function for  $q_z = 0$ , (3b) for  $q_z = 0.05$  GeV/c, and (3c) for  $q_z = 0.10$  GeV/c. All momenta in Fig. 3 are in units of GeV/c. In addition to the maximum at  $\mathbf{q} = \mathbf{0}$ , there are prominent maxima and minima at  $q_x = 2\pi/(R_1 - R_2)$ . For this case, the correlation function has minimum at  $q_x \sim 0.70$  GeV/c and a maximum at  $q_x \sim 0.14$  GeV/c. The correlation function decreases in magnitude as  $q_z$  increases.

In the case of two equal size droplets whose centers are moving with equal and opposite velocities  $\mathbf{v}_1 = -\mathbf{v}_2 = v\mathbf{e}_z$  along the beam direction ( $z$ -axis), the correlation function  $C(q)$  is

$$C(q) = 1 + \frac{e^{-(\sigma^2 + \tau^2 v^2)q_z^2 - \sigma^2 \mathbf{q}_T^2 - \tau^2 q_0^2}}{2} \left\{ \begin{aligned} & \cosh(2\tau^2 q_0 q_z v) \\ & + \cos[\mathbf{q} \cdot (\mathbf{R}_1 - \mathbf{R}_2) - q_0(T_1 - T_2) + q_z v(T_1 - T_2)] \end{aligned} \right\}. \quad (7)$$

In this case, the correlation function  $C(q)$  is characterized by an asymmetric distribution that is narrower in the  $q_z$  direction than in the transverse direction, in addition to a cosine-type modulation along the direction of the initial separation of the two droplets. The degree of the narrowing of the  $q_z$  distribution width depends on the of the emission time width  $\tau$ . We show in Fig. 4 the correlation function  $C(q)$  at  $q_0 = 0$  for two droplets with the same geometrical dimensions as those in Fig. 3 but with  $v_z \sim 1$  and  $\tau = \sigma$ . The general features of the correlation function fluctuations are similar to the static case except that the correlation function falls faster as a function of  $q_z$ , as one can observe by comparing Figs. (3c) and (4c).

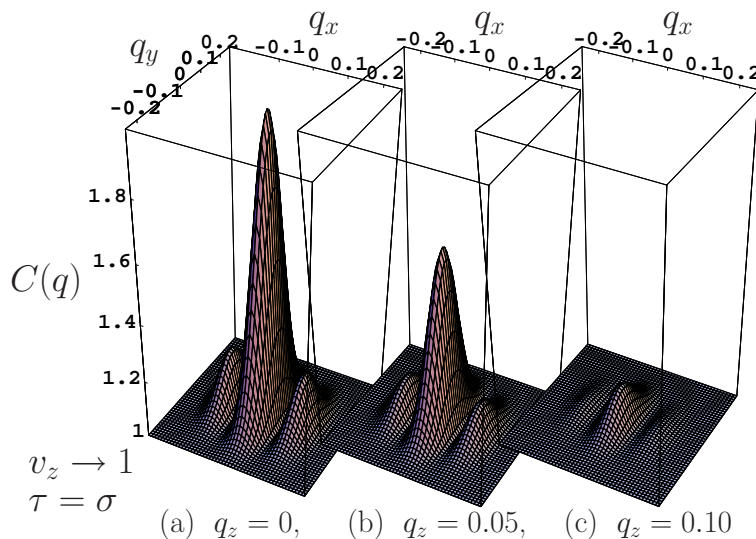


Fig. 4. The correlation function for a two droplet source with  $v_z/c = 1$  and  $\tau = \sigma$ .

In a single-event HBT measurement, one can locate the reaction plane and designate the transverse axis in the reaction plane to be the  $x$ -axis. This  $x$ -axis can be considered as the axis joining the centers of the two clusters initially. Then the correlation function will show prominent fluctuations in  $q_x$ , in addition to the Gaussian distribution in  $q_z$  and  $q_T$ , according to Eq. (7).

If the statistics of single-event is insufficient, one can perform an “aligned” multi-event HBT analysis by referring to the transverse axis in the reaction plane of each and every event as the  $x$ -axis. Then, fluctuations in  $q_x$  in different events are event-independent and will be retained. A multi-event analysis with the properly aligned transverse axis will exhibit large fluctuations as those shown in Figs. 3 and 4 and indicated by Eq. (7).

On the other hand, one can use an “unaligned” multi-event HBT analysis in which we do not align the transverse axis on the reaction plane as the  $x$ -axis,  $\mathbf{R}_1 - \mathbf{R}_2$  from different events can be considered randomly oriented in the transverse

plane. If the emission time  $T_i$  are the same, then the cosine term in Eq. (7) will be averaged to zero, and the correlation function becomes

$$C(q) = 1 + \frac{e^{-(\sigma^2 + \tau^2 v^2)q_z^2 - \sigma^2 q_T^2 - \tau^2 q_0^2}}{2} \cosh(2\tau^2 q_0 q_z v). \quad (8)$$

One can extract the radii  $R_i$ (HBT) from this type of “non-aligned” multi-event HBT analysis at  $q_0 \sim 0$ , corresponding approximately to the inverse of the coefficient of  $q_i^2$  in the exponential factor in Eq. (8), and one obtains

$$R_x = R_y = R_{\text{side}} = \sigma, \quad \text{and} \quad R_{\text{long}} \sim \sqrt{\sigma^2 + \tau^2 v^2}, \quad (9)$$

$$R_{\text{long}}/R_{\text{side}} \sim \sqrt{\sigma^2 + \tau^2 v^2}/\sigma. \quad (10)$$

This ratio is always greater than unity. Thus, while the single-event and the aligned multi-event analyses provide information on the fluctuation of the correlation function, the unaligned multi-event analysis will give the  $R_{\text{long}}/R_{\text{side}}$  ratio to provide useful information on the emission time and the relative velocity of the two clusters.

#### 4. Discussions and Conclusions

Density fluctuation occurs in high-energy heavy-ion collisions in many ways. It can arise from initial transverse density fluctuations as a result of the underlying granular structure of the colliding constituent nucleons. It can come from the non-central character of the collisions, leading to two or three clusters of pion emitting clusters. It can arise from the occurrence of first-order phase transitions. It can come from the surface tension effects which tend to form clusters of strongly-interacting matter during its evolution. The surface tension effects also lead to the multi-fragmentation of the produced matter into small clusters. Some of these density fluctuation sources are expected to be commonly present and may be detected by single-event HBT interferometry.

In a nearly head-on collision at very high energies, the number of identical pions is of the order of a few thousand. The number of observed identical pions  $n_\pi$  is a small fraction of this number. For example, the number of identical pions detected in the STAR Collaboration in the most central Au-Au collisions at RHIC is of the order of a few hundred<sup>18</sup>. Although the number of pairs of identical pions in the event varies as  $n_\pi(n_\pi - 1)/2$ , only a small fraction of these pairs have relative momenta small enough to be useful in a HBT analysis. Clearly, whether or not single-event HBT measurements can be carried out remains to be tested.

If the statistics of identical bosons turns out to be insufficient for single-event analyses using the present detectors, there remains the future prospect of performing single-event HBT analyses at RHIC with detector upgrades or with heavy-ion collisions at LHC. It will also be of great interest to carry out few-event HBT analyses by using pairs of pions in events with similar global characteristics. Because of the difference in initial conditions in different collision events, different collisions will lead to different density fluctuations for some degrees of freedom while retaining similar fluctuations for some other degrees of freedom. The use of few-event

HBT analyses may still retain those fluctuations from event-independent degrees of freedom. This may be particularly useful in the examination of two or three cluster configurations in non-central collisions by collecting events of similar impact parameters and looking at pion pairs from these events. While the single-event and the aligned multi-event analyses provide information on the fluctuation of the correlation function, the multi-event analysis will give the  $R_{\text{long}}/R_{\text{side}}$  ratio which will provide useful information on the emission time and the relative velocity of the two clusters.

### Acknowledgments

This research was supported by the National Natural Science Foundation of China under Contract No.10575024 and by the Division of Nuclear Physics, US DOE, under Contract No. DE-AC05-00OR22725 managed by UT-Battelle, LLC.

### References

1. W. N. Zhang, Y. M. Liu, S. Wang, Q. J. Liu, J. Jiang, D. Keane, Y. Shao, S. Y. Chu, and S. Y. Fung, Phys. Rev. **C51**, 922 (1995).
2. W. N. Zhang, M. J. Efaaf, and C. Y. Wong, Phys.Rev. **C70**, 024903 (2004).
3. C. Y. Wong and W. N. Zhang, Phys. Rev. **C70**, 064904 (2004).
4. W. N. Zhang, S. X. Li, C. Y. Wong, and M. J. Efaaf, Phys. Rev. **C71**, 064908 (2005).
5. W. N. Zhang, Y. Y. Ren, and C. Y. Wong, Phys. Rev. **C74**, 024908 (2006).
6. W. N. Zhang and C. Y. Wong, invited talk presented at the XI International Workshop on Correlation and Fluctuation in Multiparticle Production, Nov. 21-24, 2006, Hangzhou, China, hep-ph/0702120.
7. For a general review of the Hanbury-Brown-Twiss intensity interferometry, see Chapter 17 of C. Y. Wong, *Introduction to High-Energy Heavy-Ion Collisions*, World Scientific Publishing Company, 1994; see also Ref. [3] and references cited therein.
8. M. Naraschewski and R. J. Glauber, Phys. Rev.**A59**, 4595 (1999).
9. J. Vianna Gomes, A. Perrin, M. Schellekens, D. Biron, C. I. Westbrook, and M. Belsley, Phys. Rev. **A 74**, 053607 (2006), and references cited therein.
10. H. J. Drescher, F. M. Liu, S. Ostapchenko, T. Pierog, and K. Werner, Phys. Rev. C **65**, 054902 (2002).
11. Y. Hama, Rone P.G. Andrade, F. Grassi, O. Socolowski Jr, T. Kodama, B. Tavares, S. S. Padula, Nucl. Phys. **A774**, 169 (2006).
12. O. Socolowski Jr., F. Grassi, Y. Hama, and T. Kodama, Phys. Rev. Lett. **93**, 182301 (2004);
13. L. D. Landau, Izv. Akad. Nauk. SSSR. ser. fiz. **17**, 51 (1953); L. D. Landau and S. Z. Belenkii, Usp. Fiz. Nauk **56**, 309 (1955).
14. C. Y. Wong, Ann. Phys. (N.Y.) **77**, 279 (1973).
15. E. Witten, Phys. Rev. D **30**, 272 (1984).
16. S. Pratt, P. J. Siemens, and A. P. Vischer, Phys. Rev. Lett. **68**, 1109 (1992); L. P. Csernai and J. I. Kapusta, Phys. Rev. **D46**, 1379 (1992); L. P. Csernai and J. I. Kapusta, Phys. Rev. Lett. **69**, 737 (1992); R. Venugopalan and A. P. Vischer, Phys. Rev. **E49**, 5849 (1994).
17. J. Rizzo, M. Colonna, A. Ono, nucl-th/0609053); Ph. Chomaz *et al.*, Phys. Rept. **389**, 2632004 (2004).
18. J. Adams *et al.*, the STAR Collaboration, nucl-ex/0311017.